Supporting Information

Meer et al. 10.1073/pnas.1116269109

SI Materials and Methods

Constructs were generated by inserting PCR-generated fragments containing T7 promoter–5′ linker–iR4 or iR4-Zipper or iR4-RTR–3′ linker with an RT primer binding site into the pUC19 vector between HindIII and XbaI restriction sites. Cloned plasmids were linearized with XbaI and used as templates for in vitro transcription (Ambion). Transcriptions were purified on an 8% denaturing polyacrylamide gel (29:1 acrylamide:bis-acrylamide, 7 M Urea). The RNA was resuspended in 0.5× Tris-EDTA (TE) buffer. RT primer oligos (Operon) were labeled using γ[^{32}P] ATP and polynucleotide kinase and purified using G-25 MicroSpin columns (GE Healthcare). *N*-methylisatoic anhydride (NMIA) modification of RNA followed the method of Wilkinson et al. (1), except that we used 12 pmol of RNA. RNA was treated with 13 mM NMIA in DMSO or DMSO alone for 45 min at 37 °C, then ethanol precipitated and reverse transcribed. Sequencing reactions were analyzed using a 12% denaturing polyacrylamide gel (7 M Urea). The gel images were produced using a Typhoon phosphorimager (GE Healthcare). Analysis and quantification were carried out using the SAFA program (2). Band intensities in the NMIA (−) lane were subtracted from the (+) lane to determine the selective 2'-hydroxyl acylation analyzed by primer extension (SHAPE) (NMIA) reactivites, and the highest degree of NMIA modification was set to 100%.

1. Wilkinson KA, Merino EJ, Weeks KM (2006) Selective 2′-hydroxyl acylation analyzed by primer extension (SHAPE): Quantitative RNA structure analysis at single nucleotide resolution. *Nat Protoc* 1:1610–1616.

2. Das R, Laederach A, Pearlman SM, Herschlag D, Altman RB (2005) SAFA: Semi-automated footprinting analysis software for high-throughput quantification of nucleic acid footprinting experiments. *RNA* 11:344–354.

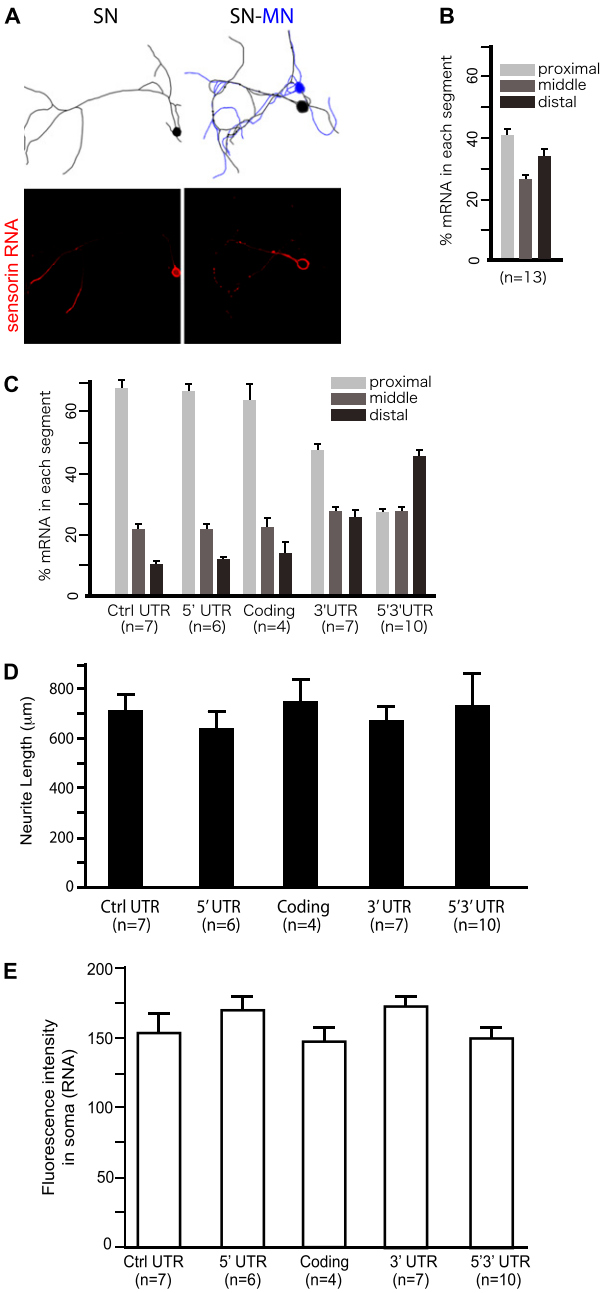

Fig. S1. Related to Figs. 1 and 2. (*A*) Localization of endogenous sensorin mRNA in isolated sensory neurons (SNs) and SNs cocultured with target motor neuron (MN). Upper: Neuronal morphology traced from differential interference contrast images of cultured SNs and MNs [day in vitro (DIV) 4]. Black, SN; blue, MN. *Lower*: FISH of endogenous sensorin mRNA. Note that sensorin mRNA is diffusely localized in distal neurites of isolated SNs but concentrated at varicosities in SNs cocultured with target (LFS) MNs. (*B*) Quantification of sensorin mRNA localization in isolated SNs quantified as percentage of mRNA FISH intensity in proximal, middle, and distal neurites. (*C*) Quantification of reporter mRNAs FISH intensity in the proximal, middle, and distal neurites in isolated sensory neurons (DIV 4; these data complete the data presented in Fig. 1; see Fig. 2*D* for quantification of synaptic localization of sensorin mRNA). (*D*) Average length of sensory neurites is similar across groups analyzed. This indicates that expression of the various reporters does not alter neuritic growth. (*E*) Mean intensity of FISH signal in the soma is similar across groups analyzed. This indicates that the various reporters are expressed at relatively similar levels.

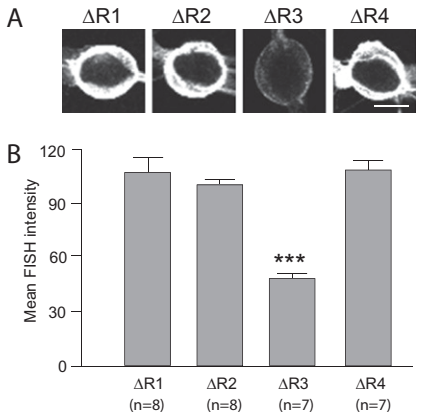

Fig. S2. Expression level of deletion mutants, related to Fig. 3. (*A*) Confocal images of somatic FISH signals for ΔR1–4 in SN–MN cultures. (*B*) Quantification of fluorescence intensity of dendra2 FISH intensity. Only ΔR3 shows decreased RNA concentration, yet this construct retained synaptic localization.

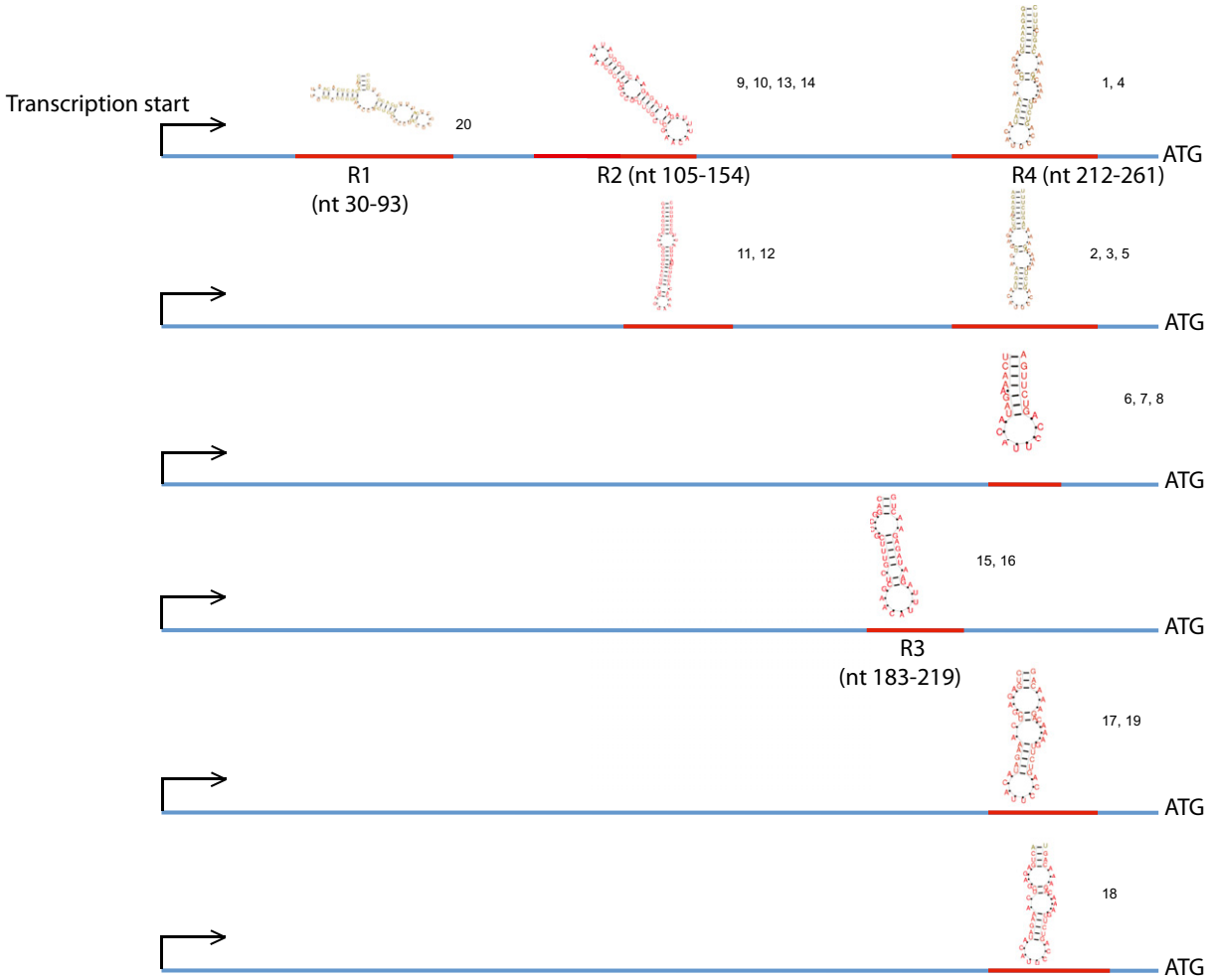

Fig. S3. Secondary structures predicted using RNApromo (1) and their corresponding regions within the sensorin 5′ UTR. RNApromo was used in the initial screen for secondary structure(s) within the 5′ UTR. Relevant to Figs. 3 and 4. A total of 20 candidate secondary structures were predicted using RNApromo software, numbered 1 through 20. The structures that were located in the same region (red line) and that shared similar secondary structures were clustered together, and a representative structure is displayed (e.g., structures with probability color code variation). After further secondary structure analysis with RNAfold (2), R1–4 were chosen for the initial deletion screening analysis; the numbers in parentheses denote the specific positions of R1–4 within the 5′ UTR of sensorin.

1. Rabani M, Kertesz M, Segal E (2008) Computational prediction of RNA structural motifs involved in posttranscriptional regulatory processes. *Proc Natl Acad Sci USA* 105:14885–14890.
2. Gruber AR, Lorenz R, Bernhart SH, Neuböck R, Hofacker IL (2008) The Vienna RNA websuite. *Nucleic Acids Res* 36(Web Server issue):W70–W74.

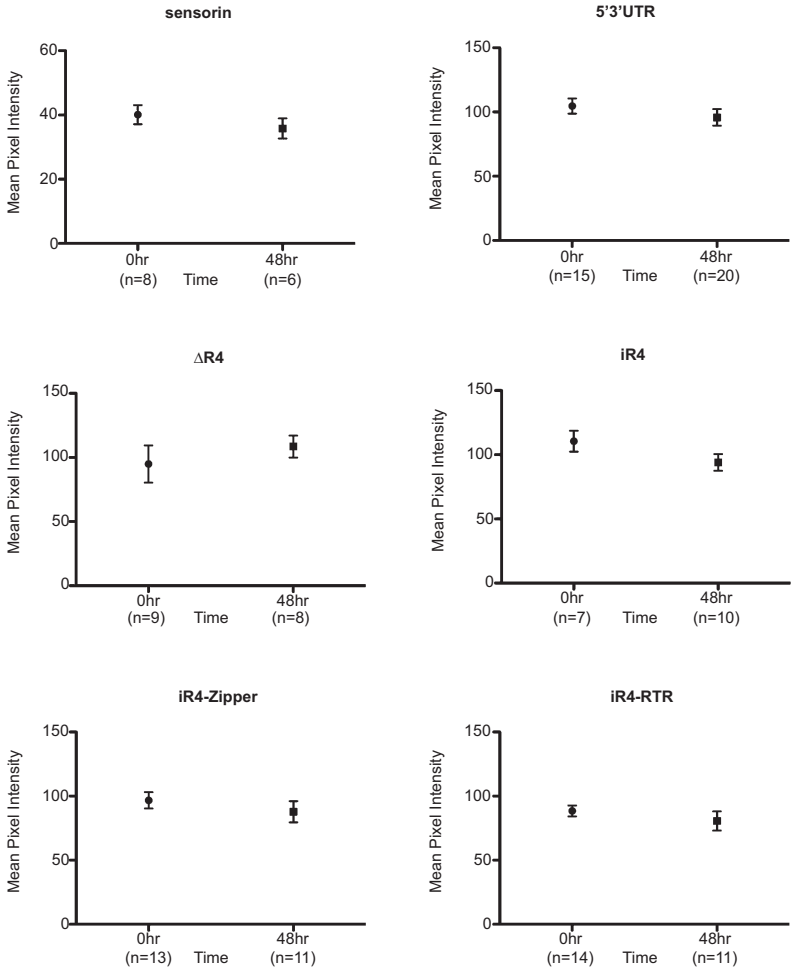

Fig. S4. Endogenous sensorin and reporter RNAs are stable in isolated neurites. The stability of endogenous sensorin and select reporter RNAs was measured by injecting isolated sensory neurons (DIV 1) with pNEX vectors encoding sensorin reporters. Cell bodies were mechanically removed 48 h later, and neuritis were fixed at either 0 or 48 h after soma removal and processed for FISH. Images were analyzed to determine the mean pixel intensity for each cell. The concentration of endogenous sensorin and of all reporter RNAs did not decrease significantly between 0 and 48 h. Student *t* test. *n*, number of cells analyzed.

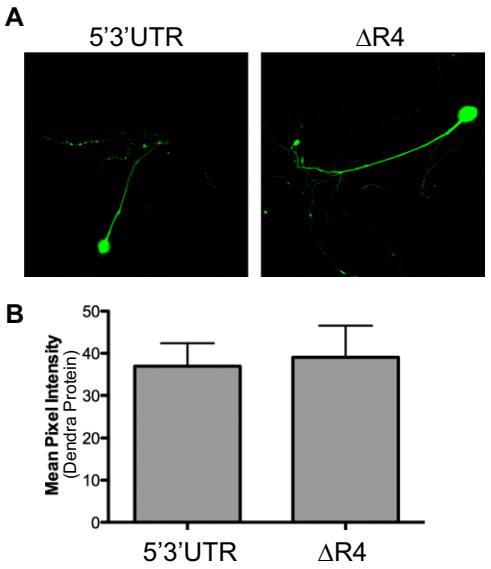

Fig. S5. Deletion of the synaptic localization element does not alter dendra2 protein concentration, related to Fig. 3. (*A*) Representative confocal images of dendra2 protein (green) in sensory neurons (paired with motor neurons) expressing the 5′3′ UTR reporter or the ΔR4 reporter. (*B*) Quantification of mean pixel fluorescence intensity of dendra2 protein; Student *t* test, ns.

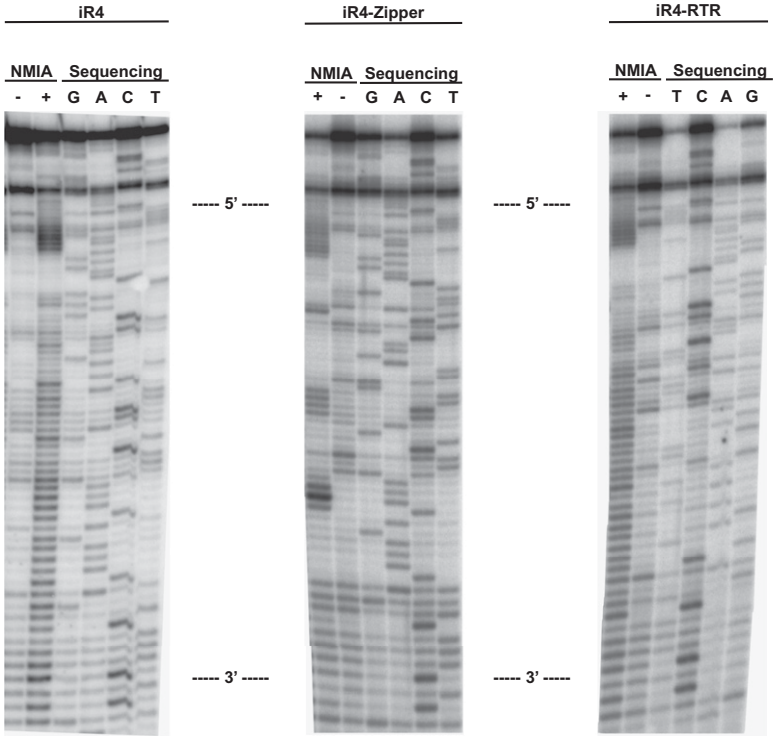

Fig. S6. SHAPE polyacrylamide gels. Sequencing polyacrylamide gels for SHAPE (1) analysis of the RNA (from 5′ to 3′, as denoted). The lanes marked sequencing are lanes in which ddNTPs were added to the reverse transcription to cause chain termination and are exactly 1 nt longer than the corresponding NMIA lanes. NMIA lanes (+) and (-) correspond to incubation with 130 mM NMIA for 45 min at 37 °C and a control with NMIA omitted. Unbased paired segments are visible as regions of increased NMIA modification in the (+) lane compared with the (-) lane.

1. Wilkinson KA, Merino EJ, Weeks KM (2006) Selective 2′-hydroxyl acylation analyzed by primer extension (SHAPE): Quantitative RNA structure analysis at single nucleotide resolution. *Nat Protoc* 1:1610–1616.